

Merlin

# MerlinEM

## Application Note

Using 4D-STEM to measure electromagnetic fields in the transmission electron microscope

### Key methods:

- Differential Phase Contrast (DPC)
- Centre of Mass (CoM)
- Cross-correlation (CC)

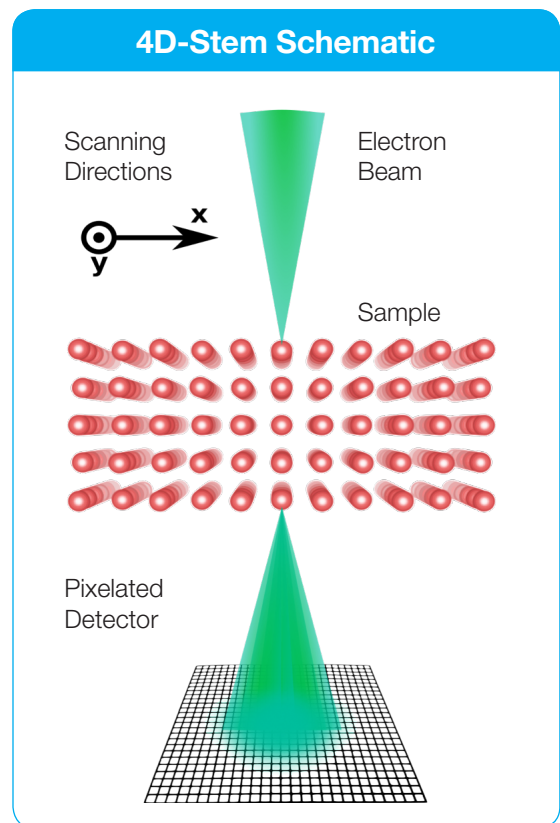
**MerlinEM is a fast electron counting pixelated detector for the transmission electron microscope. Its dynamic range, radiation hardness and versatile readout system make it an exciting tool for scientific research.**



MerlinEM can be used as a 4D-STEM camera where a full diffraction pattern is acquired at each point in a scan. Applications of 4D-STEM imaging are wide ranging; established methods including bright field imaging (BF), high angle annular dark field imaging (HAADF), annular bright field imaging (ABF) and differential phase contrast (DPC) are easily accessible through post processing. Exciting emerging techniques like ptychography, momentum transfer imaging and pattern matching would not be possible without access to the full diffraction information enabled by pixelated detectors like MerlinEM. A selection of open source software is available for analysis of 4D-STEM and MerlinEM data<sup>1</sup>.

**Key specifications:** noiseless readout; no dead time with 1-bit (14400 fps), 6-bit (2400 fps) or 12-bit (1200 fps) imaging; 30 keV - 300 keV operation; pixel size 55 x 55 μm; active area: 14 x 14 mm (256 x 256 pixels) or 28 x 28 mm (512 x 512 pixels); DQE at 60 keV: 1 at Zero frequency, 0.45 at Nyquist; MTF at 60 keV: >0.62 at Nyquist.

<sup>1</sup> LiberTEM <https://libertem.github.io/LiberTEM/index.html>  
 HyperSpy <https://hyperspy.org/>  
 pixelatedDPC <https://github.com/matkrj/pixelatedDPC>  
 pixSTEM <https://pixstem.org/index.html>  
 py4DSTEM <https://github.com/py4dstem/py4DSTEM>  
 fpd <https://gitlab.com/fpdpy/fpd>



This note will focus on quantitative imaging of electromagnetic fields in the transmission electron microscope in scanning mode. Electromagnetic fields can be separated into two length scales:

## 1. Nanobeam diffraction

In nanobeam diffraction mode, where diffracted beams do not overlap, transmitted electrons will be deflected due to the Lorentz force:

$$\mathbf{F} = -e\mathbf{E} - e(\mathbf{v} \times \mathbf{B}),$$

where  $e$  is the charge of an electron,  $\mathbf{E}$  is the electric field,  $\mathbf{v}$  is the speed of the electron and  $\mathbf{B}$  is the magnetic induction. Transmitted electrons acquire momentum which is integrated over the thickness of the sample.

In this part we focus on imaging of magnetic fields, however, essentially the same methodology can be used to analyse long-range electric fields in e.g. biased sample with a PN junction.

In the case of magnetic fields, the measurement is only sensitive to the component of the field perpendicular to the electron trajectory. It is also important to mention that the vast majority of magnetic samples need field free conditions, otherwise the magnetisation of the sample is saturated in the high field created by the objective lens of the TEM. This additional momentum results in a shift of the central probe (disk) on a detector, which can be measured quantitatively.

Quadrant and annular quadrant detectors are the established detection methods for measurement of the disk shifts. In the case of MerlinEM, multiple opportunities for signal analysis are available. We can process the data with virtual DPC and annular DPC detectors, allowing quick analysis but sacrificing most advantages of having the full diffraction information available at each point in a scan. The convenience of this approach is that we can define a suitable detector geometry and its centre post experiment.

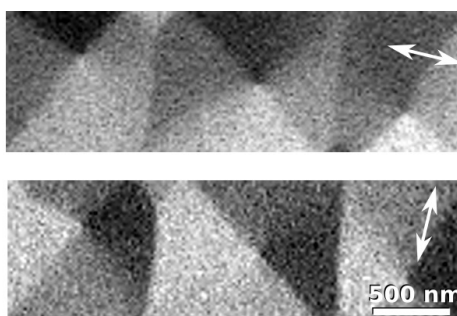
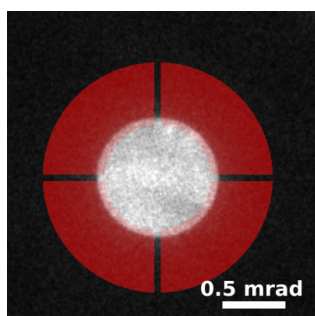


**Fig 1:** (Left) image of diffraction pattern with a virtual four quadrant annular detector overlaid. (Right) The result of analysis of probe shifts from virtual detector specified on left. The sample was 8 nm thick Ni<sub>80</sub>Fe<sub>20</sub>. Two images are two orthogonal deflections of the beam with arrows specifying the orientation of the magnetic field components.<sup>2</sup>

Fast acquisition, electron counting and noise-less readout make MerlinEM an ideal tool for dynamic TEM imaging. Timescales below 100 ns are reported in pump probe experiments<sup>3</sup>. Imaging of in-situ dynamic processes with up to 2400 fps is possible with 6-bit dynamic range. In the case of EM fields, TEM can be used in fresnel mode (defocused illumination) to image fast field dynamics. MerlinEM can be also used in a binary mode with up to 14400 fps with individual frames acquired in 70  $\mu$ s.

2 Ni<sub>80</sub>Fe<sub>20</sub> sample was made by Azzawi Sinan and Del Atkinson from University of Durham, UK.

3 Patterson G.W. et al, preprint <https://arxiv.org/abs/1905.11884>

4D-STEM data can be also used to calculate the Centre of Mass (CoM) of the pattern on the detector. This method has an advantage in that the shift of the probe is measured linearly - contrary to the quadrant method, where the selection of the centre of the pattern is important and the beam shifts have to be within a certain range.

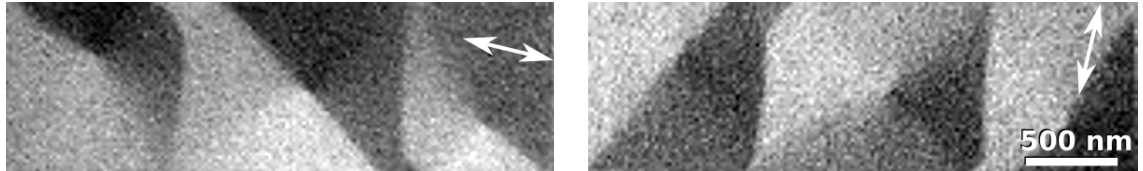


**Fig 2:** Centre of mass generated image from the sme dataset as the image above. The small discrepancies in signal between FIG 1 and FIG 2, calculated with different methods, are artefacts related to imperfect placing of the virtual detector in the quadrant method.

A lot of industrially relevant research is applied to polycrystalline materials, for which the CoM method might not be the ideal approach. This can happen if the size of the features (crystalline grains) is comparable to the size of the beam. Under these conditions, the intensity in the central diffraction disk is not flat but has variations due to crystallites meeting different diffraction conditions. Therefore, with CoM and quadrant based approaches the final image also contains diffraction contrast which is not related to the deflection of the probe. This is overcome by a method based on computer vision, where the probe position is analysed by a template matching algorithm. Each diffraction pattern in 4D-STEM dataset can be cross-correlated with an idealised mask pattern. To achieve even greater signal to noise, a 2D gradient is applied to the data before cross-correlation. This way we can achieve a superior imaging mode, which isolates the magnetic contrast from the short-range electrostatic crystallite contrast.

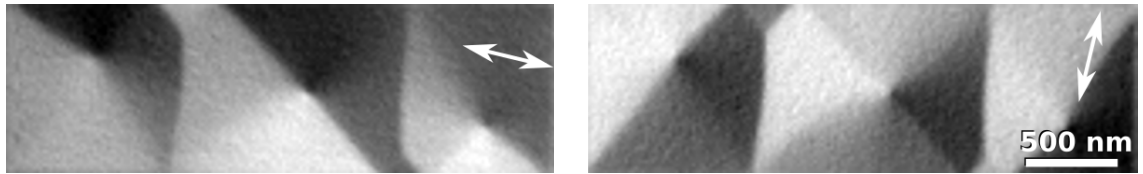


**Fig 3:** Cross-correlation (CC) based analysis of the same 4D-STEM dataset. The superior contrast of the CC method is evident when compared with Figs 1 and 2. The analysis code is based on GPU acceleration and is freely available<sup>4</sup>. The details about processing and methodology can be found in Krajnak M. et al, Ultramicroscopy 2016.

Even very complicated samples (e.g. perpendicularly magnetised multilayer polycrystalline films) can be quantitatively imaged with the cross-correlation method. An example of such an image is shown below.

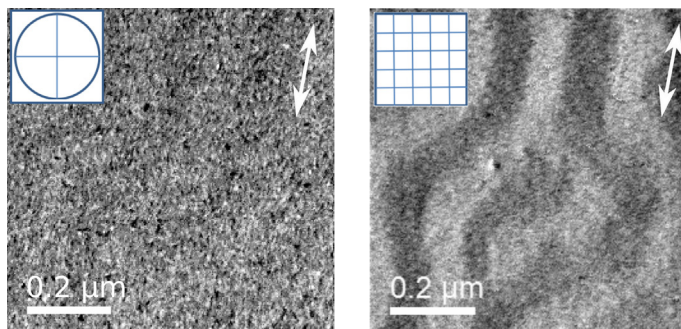


**Fig. 4:** A comparison of magnetic field images from segmented (left) and cross-correlation (right) methods. The sample consists of 15 repeated layers of [Co(1.6)|Ru(1.4)|Pt(0.6)] capped with Pt(2.4) on the top and Ta(10)|Pt(8) on the bottom (number in brackets is the thickness of the given layer in nanometres). In such a complicated structure DPC detection shows no magnetic contrast at all and only cross-correlation can be used. In this case the sample is magnetised out of plane so it needed to be tilted to show any contrast. It is remarkable that even if the effective magnetic thickness is only 17% of the thickness of the sample, the contrast can be still recovered in a multilayered polycrystalline structure. Image courtesy Kayla Fallon, details can be found in Fallon K. et al, preprint <https://arxiv.org/abs/1901.03652>.

4 pixelatedDPC <https://github.com/matkraj/pixelatedDPC>

## 2. Atomic scale electric fields

Electric fields can also be measured on atomic scales with MerlinEM. It was shown that an average momentum transfer from a transverse electric field can be measured by a CoM algorithm in thin samples. Momentum transfer can be described by:

$$\langle \mathbf{p}_\perp \rangle = \iint \mathbf{p}_\perp \cdot \mathbf{I}(p_x, p_y) dp_x dp_y$$

where  $\mathbf{p}_\perp$  is the average transverse momentum transferred to the beam by the sample,  $\mathbf{I}(p_x, p_y)$  is the recorded diffraction pattern (normalised) with the components representing the coordinate system in the momentum space. This equation essentially denotes a CoM calculation of the measured diffraction pattern.<sup>5</sup> In this scenario, the probe size is smaller than the atomic spacing. Even if there was a probe shift due to the long range EM fields, this shift would be overcome by effects of atomic electric fields. Probe shifts in nanodiffraction are usually in the range of tens of microradians or smaller, whereas the expected average shift for atomic resolution imaging can be close to the size of the probe defining aperture e.g. >5/10 milliradians (about 3 orders of magnitude larger).

In recent publications<sup>6,7</sup> MerlinEM was successfully used to measure atomic electric fields - a quickly developing field of research. Interestingly, once acquired, the 4D-STEM data can be used for multiple types of analysis; focused probe ptychography and atomic electric field imaging essentially require the same type of data. In the image below, 4D-STEM data of a 2D material, MoS<sub>2</sub>, was used to generate a phase image (by ptychography), a transverse electric field image (by CoM) and a charge distribution image (by divergence of CoM). Thus illustrating the richness of information available from a single dataset.

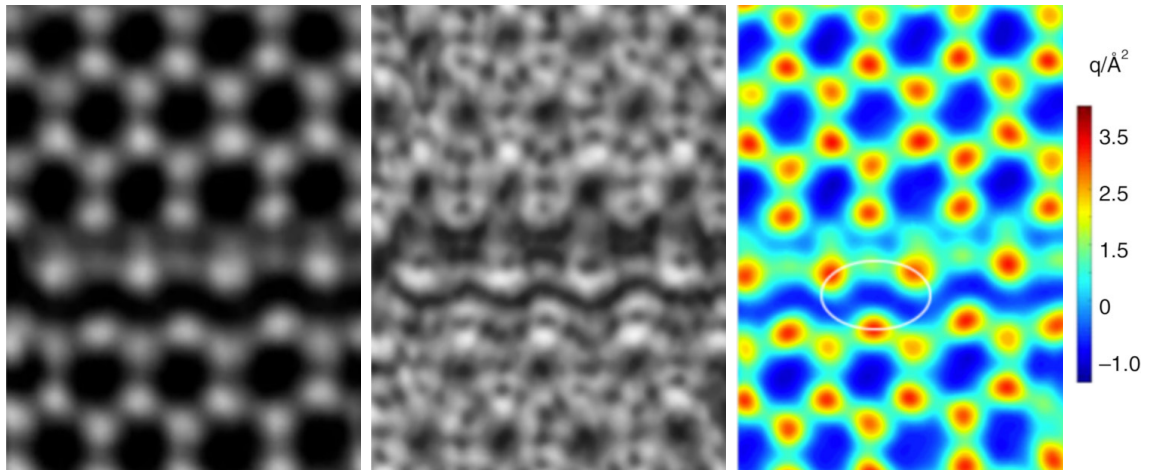


**Fig 5:** Phase (left), the magnitude of the electric field (middle) and the charge distribution (right) images generated from the same 4D-STEM dataset acquired by MerlinEM detector in MoS<sub>2</sub> with a horizontal defect present in the middle of the image. The image was obtained under CC BY 4.0 licence from Fang S. et al, Nature Communications volume 10, 1127 (2019).

5 Müller-Caspary K. et al, Nature Communications (2014)  
 6 Fang S. et al, Nature Communications volume 10, 1127 (2019).  
 7 Müller-Caspary K. et al, Ultramicroscopy, Vol 203, (2019)